Journal of Superconductivity and Novel Magnetism
https://doi.org/10.1007/s10948-021-05964-1

ORIGINAL PAPER

# Iron-Cobalt Coatings Produced Using an Eco-friendly Route

E. A. Denisova[1,2] · L. A. Chekanova[1] · S. V. Komogortsev[1] · I. V. Nemtsev[2,3] · R. S. Iskhakov[1] · M. V. Dolgopolova[2]

Received: 9 June 2021 / Accepted: 28 June 2021


**Abstract**
A facile, low-cost, and green route for synthesis of high-induction Fe–Co coatings was developed. Within this approach, three natural reducing agents have been used for deposition of the metal coatings by electroless plating on dielectric and metallic substrates: arabinogalactan, starch, and sucrose. The Fe–Co alloy coatings with Co content from 0 to 94 at.% are nanocrystalline bcc solid solution with carbon additive no more than 2 at%, and pure Co coatings are of hcp structure. The magnetic properties of bcc-based iron–cobalt alloys have been investigated as a function of the atomic composition. A high-saturation magnetization of about 240 emu/g was obtained for $Fe_{70}Co_{30}$ alloy films deposited onto copper substrate. The local magnetic anisotropy of FeCo alloys increases with a decrease in iron content for all reducing agents. High magnetization close to those in the bulk Fe–Co alloys implies the prospective applications of synthesized Fe–Co coatings as magnetic shield and magnetic sensors.

**Keywords** High-induction Fe–Co coating · Electroless deposition · Structure · Magnetic properties · Eco-friendly synthesis

## 1 Introduction

Iron–cobalt (Fe–Co) bimetallic alloys attract much interest due to their potential applications as material bases of magnetic sensors and data storage devices [1–4]. The CoFe alloy films exhibit superior magnetic properties such as high Curie temperature and high saturation magnetization $M_S$ (up to 245 emu/g) [5, 6]. There are many ways for the FeCo soft magnetic alloy fabrication such as electroplating, sputtering, electroless plating, mechanical alloying, and molecular beam epitaxy [7–13]. Vacuum processes have a low productivity effect, so these ways are hard to be applied in industry. Electroless plating shows low cost and no size or shape limit for the preparation of nanoscale films. On the one hand, electroless deposition represents a simple, cost-effective way of fabricating FeCo coatings. However, the use of conventional reducing agents (sodium hypophosphite or borohydride, hydrazine) leads to significant contaminations with phosphorus and boron in deposited coatings damaging the magnetic performance (for example, a saturation magnetization value is decreased [14, 15]). Also, traditional reducing agents are often toxic.

There is a growing need to prepare environmentally friendly magnetic materials that do not produce toxic wastes in their process synthesis protocol. Green reducing agents, on the other hand, are generally derived from renewable resources and biodegrade to innocuous, often a naturally occurring product. So, researchers found that polysaccharides (e.g., chitosan, cellulose, arabinogalactan) could be an efficient, low-cost, and environmental alternative to conventional reducing agents [16–18]. However, it is not easy to control the growth and morphology of FeCo thick films. The morphology and microstructure, which affect the magnetic properties of FeCo films, are often determined by the deposition conditions such as the pH value, temperature, and addition agents [19]. Due to increasing storage capacities, there is a need to improve the properties of the magnetic layers, and grain size reduction seems to be a promising way to tailor the properties of the deposits [20]. We have previously demonstrated the possibility of obtaining thin Fe–Co films by green chemistry technique [21]. These results are, however, still insufficient for producing FeCo coatings with predictable magnetic properties because of the lack of a systematic investigation of the effect of the electroless plating conditions on deposit structure, morphology, and magnetic properties.

✉ E. A. Denisova
len-den@iph.krasn.ru

[1] Kirensky Institute of Physics, Federal Research Center KSC SB RAS, Krasnoyarsk 660036, Russia

[2] Siberian Federal University, Krasnoyarsk 660041, Russia

[3] Scientific Center, Federal Research Center KSC SB RAS, Krasnoyarsk 660036, Russia

Published online: 19 July 2021

In this work, we have developed a facile, environmentally friendly, and highly efficient method for fabricating nanostructured FeCo thick films. The FeCo coatings produced by electroless deposition with carbohydrates have a better morphology and higher $M_s$ than those for films prepared with conventional reducing agents [21]. We have used carbohydrates as reducing agents for the synthesis of FeCo films. Also, we have used nontoxic reactants and solvents. The aim of this work is to investigate the effect of the deposition conditions on the chemical composition, structure, and magnetic properties of FeCo coating. In addition, we demonstrated a strong influence of the coating composition on its magnetic anisotropy. Magnetic studies of these films which exhibit high saturation magnetization are also reported in this work.

## 2 Experimental Procedure

### 2.1 Electroless Deposition of FeCo Alloy

The FeCo–C coatings were deposited on glass or Cu substrate by electroless reduction of metals from aqueous solutions of the corresponding salts. We used the method of contact plating for enhancing the electroless deposition. Copper plates contacted with the Al plate were used as a substrate. As a pretreatment before electroless plating on the glass substrate without Al contact, the substrate was treated with an $SnCl_2$ solution and subsequently with a $PdCl_2$ solution used as a nucleating agent. Each plating bath comprised of source metal ion ($CoSO_4{\cdot}7H_2O$ and $Fe(NH_4)_2(SO_4)_2{\cdot}6H_2O$ ammonium iron(II) sulfate, or Mohr's salt), complexing agent (sodium citrate $Na_3C_6H_5O_7$), chelating agent (edetate disodium $C_{10}H_{14}N_2Na_2O_8$), and reducing agent. We used several types of carbohydrates as reducing agents: arabinogalactan–natural polysaccharide (series A), corn starch–$(C_6H_{10}O_5)_n$ (series B), and sucrose–$C_{12}H_{22}O_{11}$ (series C). The pH value was adjusted by adding $NH_4OH$ solution. The cobalt sulfate concentration was adjusted to produce FeCo deposits with various cobalt contents. The bath temperature was kept at 80 °C, and no stirring action was taken during the plating. The thickness of deposited coatings was in the range of 0.6–3 μm. For comparison, the FeCo coatings were produced by electroless deposition with a sodium hypophosphite as a reducing agent. Attention should be paid to one important feature inherent in the method of chemical deposition (electroless plating) of metal films: reduction of hypophosphite to elemental phosphorus or carbohydrates to elemental carbon always occurs simultaneously with metal reduction. Thus, definite phosphorus or carbon admixture is always present in the resulting metal deposits.

### 2.2 Characterization

The magnetic and structural properties of the composite materials are characterized by electron microscopy, X-ray diffraction, and vibrating sample magnetometry. The morphological characteristics and the elemental composition of the investigated materials were analyzed using scanning electron microscopes (S5500 and TM4000 Hitachi equipped with an energy-dispersive X-ray microanalyzer (EDX)). A structural analysis of the studied systems was carried out using X-ray diffraction (Cu-Kα, $\lambda = 0.154056$ nm). TEM (Hitachi HT7700) observations were performed on the cross sections of deposits. The average grain size of crystallites was calculated using the Scherrer formula according to the XRD peak broadening. The grain size of the CoFe deposits was also determined using electron microscopy. X-ray photoelectron spectra (XPS) were acquired using a SPECS (Germany) spectrometer equipped with a PHOIBOS 150 MCD-9 analyzer. Microwave absorption spectra were measured at 9.4 GHz. X-band FMR spectra were recorded using a Bruker spectrometer. Information on local anisotropy field $H_a$ is obtained from the investigation of approach magnetization to saturation law.

## 3 Results and Discussion

To obtain preliminary information about the deposition processes, we evaluated the dependence of the Fe content in the as-plated films on the amount of the $Fe(NH_4)_2(SO_4)_2{\cdot}6H_2O$ in the bath. Figure 1 shows the Fe content of the electroless plated Fe–Co films produced with a different type of reducing agents as a function of the amount of Mohr's salt in the bath. As expected, iron content in the film is increased

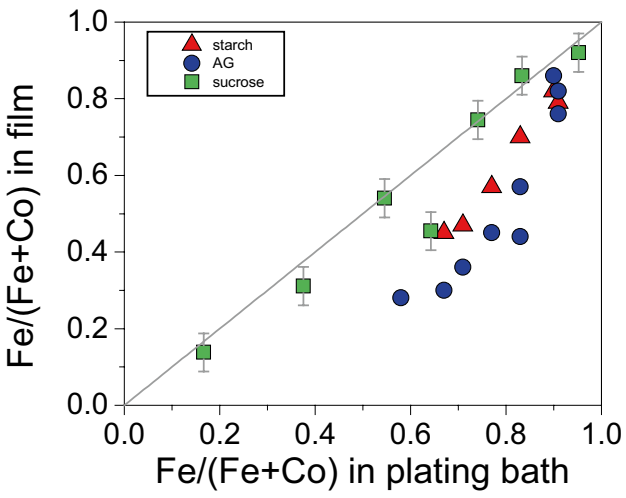


**Fig. 1** Dependence of FeCo film composition on the bath composition for different reducing agents

when the metallic ratio $Fe(NH_4)_2(SO_4)_2{\cdot}6H_2O/(CoSO_4{\cdot}7H_2O + Fe(NH_4)_2(SO_4)_2{\cdot}6H_2O)$ increases. A linear relationship of Fe (Fe/(Fe + Co)) in films and bath solution was obtained only for series C samples (Fig. 1). When sucrose is used as a reducing agent, the composition of the deposits closely reflects the solution composition; while we use arabinogalactan or starch as a reducing agent, the deposited films become Co-rich. Iron has a lower reduction potential than cobalt. Therefore, the results for sucrose indicate a slightly anomalous depositing behavior. Such behavior is well established in studies of electrodeposited processes [22]. The behavior is as normally expected for A and B sample series since the more noble metal (Co) is deposited preferentially; as a result, deposited films contain more Co than the bath composition.

Therefore, the composition of the Fe–Co films is adjustable by the change in the amount of Mohr's salt. The glycosidic bonds forming the carbohydrate molecules are stable at a low temperature. However, the synthesis of FeCo films was carried out at bath temperature 80 °C in an alkaline medium. The carbohydrate degradation occurs at the ends of the molecules under such conditions [23]. Aldehyde groups at the ends of molecules have reduction properties. Thus, the monosaccharide unit is separated and then oxidized to a carboxylic acid. Therefore, it can be assumed that the formation of a metal film is due to the decomposition of the carbohydrates. This assumption is confirmed by the presence of carboxyl group lines in the X-ray photoelectron spectra. According to the results of X-ray photoelectron spectroscopy studies, carbon concentration in FeCo(C) alloy does not exceed ~ 2 at% for all film series.

Representative XRD spectra of the samples fabricated by electroless plating are shown in Fig. 2. CoFe alloys can exist in three distinct phases, namely, the $\varepsilon$(hcp), $\gamma$(fcc), and $\alpha$(bcc) phases at room temperature [24]. The XRD patterns of FeCo coatings for all carbohydrates revealed peaks that perfectly matched with those of the bcc phase of CoFe (JCPDS 49–1567) or fcc-Cu substrate. All deposits were seen to have similar crystallographic structures at the same peak positions. Figure 2b shows the XRD patterns for FeCo coatings (series A) with different iron contents. The diffraction patterns of pure Co and pure Fe are also shown. In these patterns, the presence of two distinct systems of diffracted spots can be seen corresponding to bcc Fe–Co alloy and fcc-Cu substrate and no oxides phases were observed within the detection limits of the X-ray diffractometer. Peak located at 27.5° can be assigned to inclusions of the graphite phase. The bcc structure is found to be stable even for coatings with a very high concentration of Co (~0.94) beyond the thermodynamically stable bcc regime for bulk $Fe_{1-x}Co_x$ alloys ($0 < x < 0.25$ [25]). The XRD pattern for the pure Co deposit exhibited the hcp crystal structure. It can be observed that the diffraction patterns change in peak locations with the addition of Fe in the films. The dependences of the lattice parameter

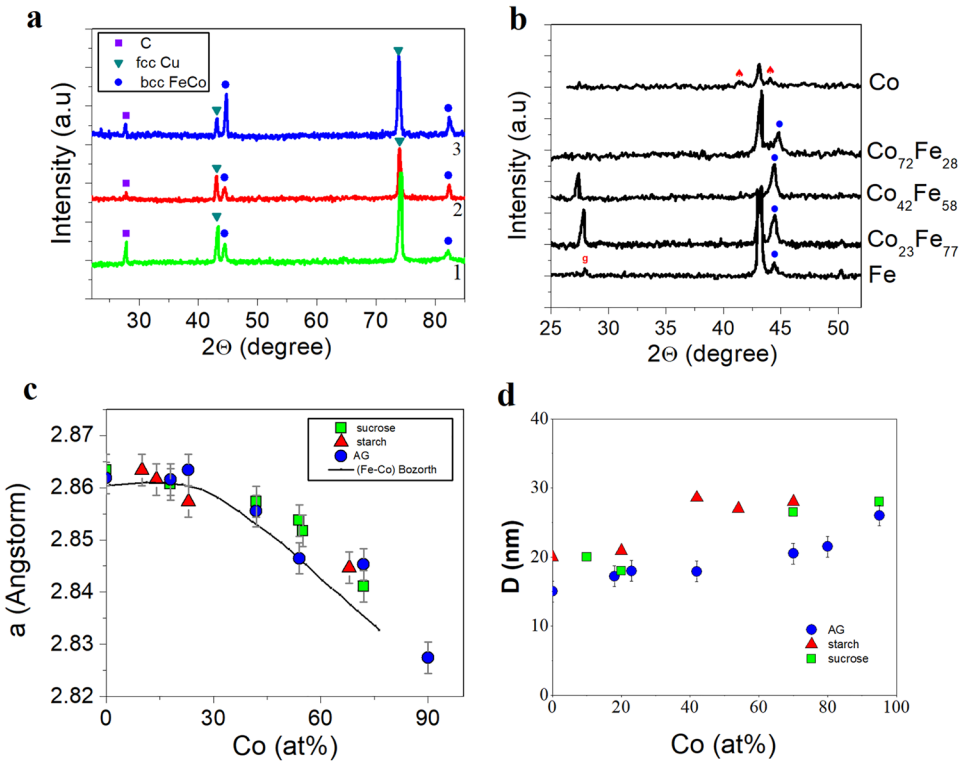


**Fig. 2** **a** XRD patterns of the $Fe_{82}Co_{18}$ films produced with different reducing agents: sucrose (1), starch (2), and arabinogalactan (3); **b** XRD patterns of the CoFe films with different iron contents (series A); **c** lattice parameter of the FeCo films as a function of the Co content; **d** the average crystallite size calculated using the Scherrer formula vs cobalt content

for FeCo films (series A) on cobalt content are shown in Fig. 2c.

The lattice constant decreases with Co content from 2.862 ($x=0$) to about 2.827 Å ($x=90$). The decrease in lattice constant $a$ with $x$ is not linear. The values of the lattice constant for the FeCo films are found to be very close to those reported for the bulk specimens [26]. The average crystallite size calculated using the Scherrer formula for all types of reducing agents was in the range of 10–27 nm. The grain size of the CoFe alloy deposits was observed to decrease with an increase in the iron content of the deposit as shown in Fig. 2d.

Figure 3 presents the TEM micrographs of the cross sections of the FeCo layer deposited with arabinogalactan as a reduced agent on Cu substrate and the EDS maps. The element mapping analysis of Fe, Co, and Cu also measured by the EDS technique reveals that Fe and Co are evenly distributed throughout the film. The diffraction pattern (Fig. 3d) confirms the formation of the bcc FeCo solid solution in the electroless deposited films.

In Fig. 4, the SEM micrographs of the cross sections of the layer deposited with arabinogalactan as reduced agent (a), starch (b), and sucrose (c) are shown. It could be observed that in all cases the grain growth is columnar, and the grains tend to arrange in columns perpendicular to the substrate surface. A similar grain structure was also observed during the investigations of CoFe electrodeposition with magnetic field [27]. The surface morphologies of the obtained samples are shown in Fig. 4d–i. It is apparent that the type of reducing agent influences the morphology. As shown in the SEM images, the surface of the FeCo film series A is much smoother than those for the FeCo film series B and C. Using arabinogalactan as a reducing agent, the surfaces of the electroless deposited films are generally smooth and uniform. But voids, pores, and cracks are occasionally observed for films deposited with sucrose. The deposition rate becomes larger when using sucrose as a reducing agent. The higher deposition rate causes a situation that there is not enough time for internal stress release and cracking of the coatings may occur. The morphology of the samples can be varied by changing the Fe/Co molar ratio (Fig. 4d–i). With an increase of Fe content in the film for all types of reducing agents, the surface morphology of the samples changed greatly. The metalized surfaces consist of agglomerates of spheroid particles for FeCo films with Fe content more than 60 at%. The grain sizes were in the range of 20–50 nm. As it is seen from Fig. 4e, h, as a result of decreasing Fe content up to 45%, a different morphology of grains is formed. In this case, we observe a 5-time increase in the grain size. Replacing carbohydrates with a conventional reducing agent (sodium hypophosphite) leads to the formation of surfaces consisting of larger, more faceted metal grains [28].

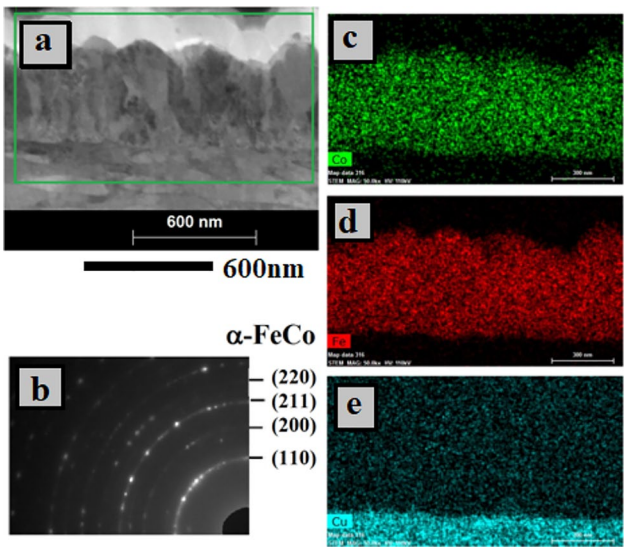


**Fig. 3** TEM cross-sectional image for the FeCo film series A (**a**); diffraction pattern for the corresponding sample (**b**); EDX element mapping images of Co (**c**), Fe (**d**), and Cu substrate (**e**)

The magnetic properties of the deposited films were determined using VSM. In Fig. 5, the normalized magnetic hysteresis loops for FeCo films deposited with different reducing agents are shown. Hysteresis loops of FeCo films are isotropic in the film plane.

It is found that films of series A are characterized by the smallest value of the local anisotropy field. The shape of the hysteresis loops leads to useful information on the factors determining the magnetic properties of samples. A homogeneous magnetic film with a field applied along with the plane displays a rectangular hysteresis loop, characterized by both large squareness ($M_R/M_S \sim 0.95$) and remanent magnetization. The investigated samples display a hysteresis loop shape atypical for films, characterized by lower squareness and remanence $M_R$. Such behavior is probably due to the columnar microstructure of FeCo films. From the comparison of the hysteresis loops shown in Fig. 5 and cross-section images shown in Fig. 3, the following observation can be made. We can see that the more pronounced is the column of microstructure, the less rectangular is the loop. Columnar growth is more pronounced in sucrose and starch (Fig. 3b, c); accordingly, the $M_R/M_S$ ratio for arabinogalactan (0.85) is higher than for starch (0.6) and sucrose (0.5).

Magnetic parameters such as saturation magnetization and the coercivity of the FeCo coatings were studied as a function of Co content. The saturation magnetization values for FeCo films produced with different reduced agents are summarized in Table 1. The data show a strong dependence of the magnetic parameters on the cobalt content. The non-monotonic behavior of the saturation magnetization $M_s$ dependencies on Co content is observed for all FeCo

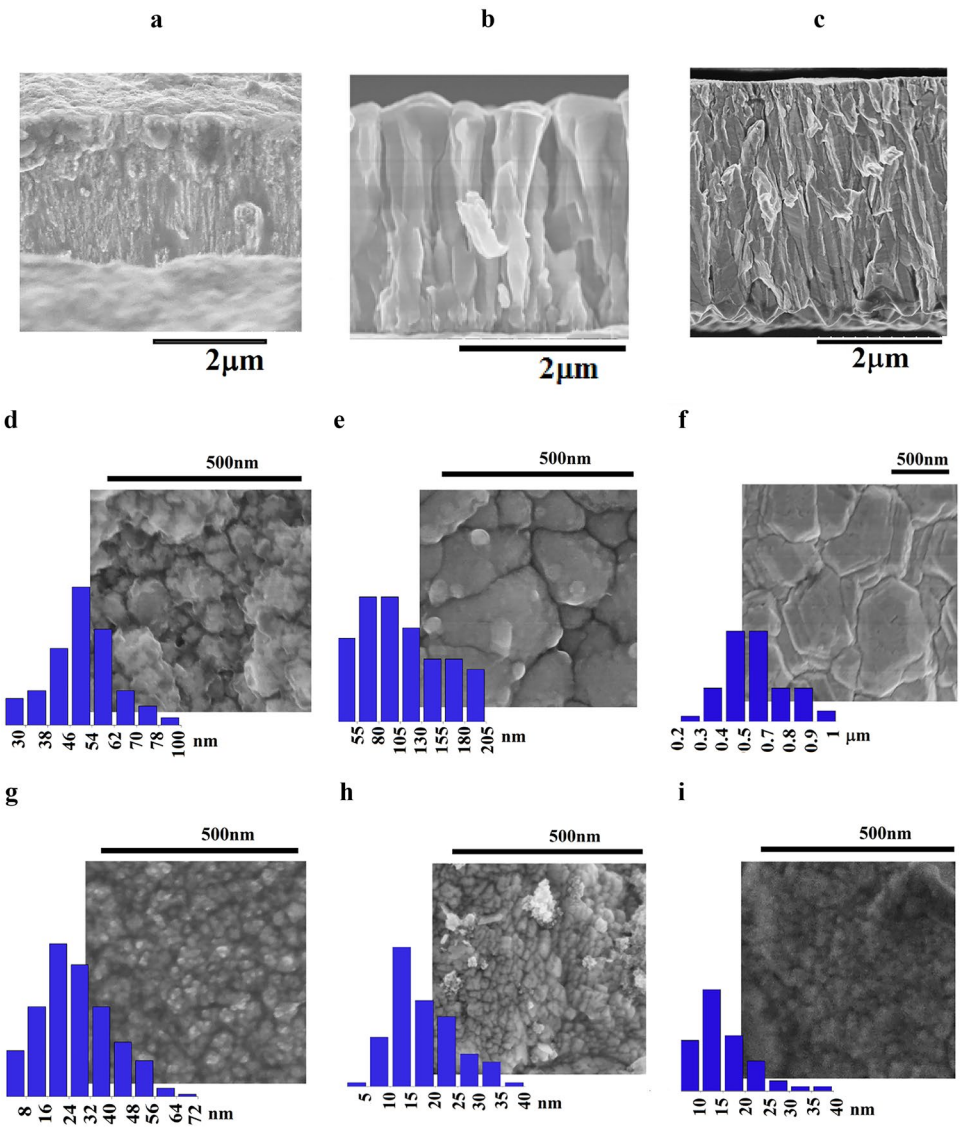


**Fig. 4** SEM images of the film cross section (**a** series A; **b** series B; **c** series C); SEM images of the surface morphology and histogram grains of the FeCo films prepared with different reducing agents and Fe contents: arabinogalactan **d** 44% Fe and **g** 82% Fe; starch **e** 14% Fe and **h** 82% Fe; sucrose **f** 14% Fe and **i** 94% Fe

film series. The maximum of saturation magnetization magnitudes is reached for the FeCo film with 30% cobalt. This result was consistent with the Slater–Pauling curve and is in reasonable agreement with a previous study for bulk and film FeCo samples [8, 26, 28–30]. The produced FeCo films demonstrated significantly better saturation magnetization values and less contamination, compared to those for the sample prepared with a conventional reducing agent (sodium hypophosphite). The $M_s$ value for film reducing with hypophosphite does not exceed 190 emu/g due to phosphorus contaminations. In cases of FeCo film reduced with carbohydrates, the $M_s$ values are 205, 235, and 240 emu/g for arabinogalactan, starch, and sucrose, respectively. The magnetization values of the samples are relatively higher than those of the usual FeCo-C alloy [31]. It is mainly due to carbon which is not included in the FeCo lattice during the deposition process.

The magnetic anisotropy field $H_a$ and $M_s$ of the film are the significant parameters for the high-frequency applications. The values of $H_a$ and $M_s$ are usually estimated from the hysteresis loops measured along with the easy axis and hard axis directions. When the hysteresis loop is not well defined with a larger squareness ratio, it is inaccurate to estimate $H_a$ and $M_s$ of film using this approach [32]. To obtain the $M_s$ and $H_a$ values of these films more accurately, experimental investigations of the ferromagnetic resonance spectra and approach magnetization to saturation law are performed. For the FMR techniques, according to Kittel's equation [33], the dependence of resonance response from the applied magnetic field can be expressed as follows:

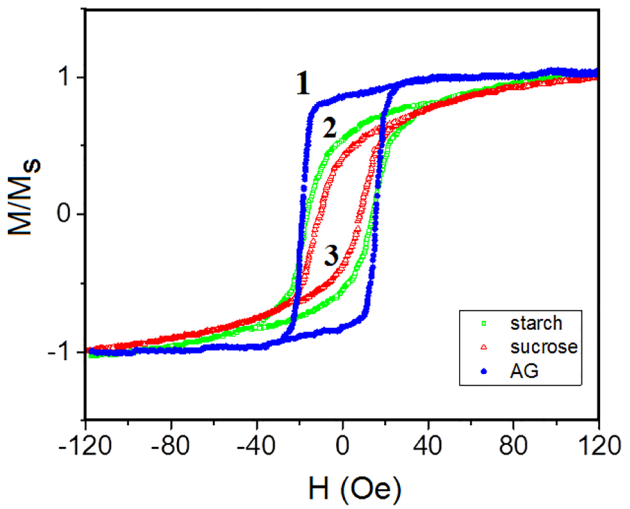


**Fig. 5** Typical M–H loops for $Fe_{77}Co_{23}$ films produced with different reducing agents: arabinogalactan (1), starch (2), sucrose (3)

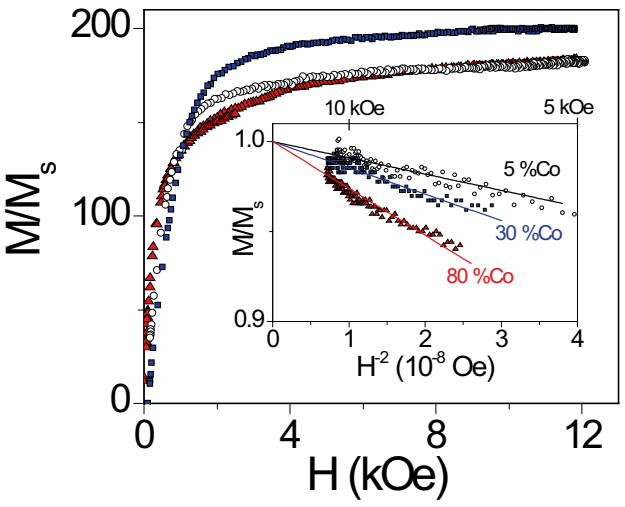


**Fig. 6** The magnetization curves for FeCo film series A with different Co contents. The insert shows approach magnetization to saturation curve for FeCo films. Thin lines represent Eq. (2) with $a=(1/15)^{0.5}$

$$\frac{\omega}{\gamma} = H_r - 4\pi M, \tag{1}$$

where $\gamma = g\mu_B/h$ is the gyromagnetic ratio, $g=2$. It was found that the $M_s$ values estimated from the FMR data are ~6% higher than that of the $M_s$ values for FeCo films determined by VSM. The differences in the $M_s$ values may be due to the fact that the weight of carbon present in the film in the form of carboxyl groups is not taken into account.

Information on local magnetic anisotropy field $H_a$ was obtained from investigation of approach magnetization to saturation law [34]. Figure 6 shows the typical experimental magnetization curves for FeCo films with different Co content. For all film series, the high-field part of magnetization curves (for H from 6 to 14 kOe) satisfies the dependence

$$M = M_s\left(1 - \left(\frac{a \cdot H_a}{H}\right)^2\right), \tag{2}$$

where $H_a = 2\,K/M_s$ is the magnetic anisotropy field, and $a$ is a coefficient equal to $(1/15)^{0.5}$ for uniaxial anisotropy and $(2/105)^{0.5}$ for cubic anisotropy. The latter enables us to determine the local anisotropy field $H_a$, which contains contributions of magnetocrystalline anisotropy and anisotropy of internal stresses. As it is seen from Fig. 7, the positive linear correlation of Co content in Fe–Co alloy and the local magnetic anisotropy field is observed. The $H_a$ value for FeCo alloys with bcc structure increases with an increase in Co content and was in the range 1.3–6 kOe. The Co coating with the hcp structure was characterized by $H_a$ ~ 7.5, 5.4, and 5.3 kOe for series B, A, and C, respectively.

**Table 1** The saturation magnetization of FeCo films produced with different reducing agents

| Reducing agent | Arabinogalactan | Sucrose | Starch | Hypophosphite | Bulk FeCo alloy [26] |
|---|---|---|---|---|---|
| Co content, at% | $M_s$, emu/g | $M_s$, emu/g | $M_s$, emu/g | $M_s$, emu/g | $M_s$, emu/g |
| 0 | 181 | 203 | 186 | 170 | 224 |
| 5 | 185 | 213 | 190 | | 229 |
| 15 | 200 | 224 | 193 | 180 | 237 |
| 30 | 205 | 240 | 235 | 190 | 243 |
| 40 | 203 | 237 | 230 | 182 | 240 |
| 50 | 200 | 230 | 226 | | 235 |
| 60 | 192 | 200 | 209 | 181 | 225 |
| 70 | 192 | 215 | 176 | | 212 |
| 80 | 180 | 198 | 160 | 160 | 194 |
| 90 | 150 | 170 | 155 | | 177 |
| 100 | 140 | 150 | 155 | 125 | 160 |

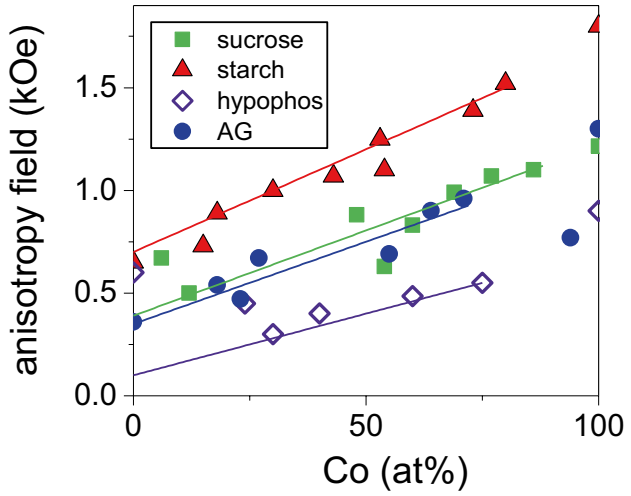


**Fig. 7** The local anisotropy field $aH_a$ of FeCo films as a function of Co content

The coercivity values range from 12 up to 25 Oe for coatings produced with carbohydrates. The best soft magnetic properties corresponded to the deposits with bcc structure and grain sizes less than 20 nm. When we use hypophosphite as a reducing agent, the lowest value of the coercive force for FeCo film is 35 Oe. In general, soft magnetic properties of films with a smooth surface are better than those for films with a rough surface, since a smooth surface does not prevent domain wall movement during magnetization. As shown in the SEM images (Fig. 4), the surface of the FeCo film A, B, and C series is much smoother than that for the FeCo film produced with hypophosphite. Zhang and Ivey [35] and Yanai et al. [6] have plated F–Co thick films by electroplating and reported the $Fe_{66}Co_{34}$ thick film with a coercivity of 16 Oe and 25 Oe for the $Fe_{76}Co_{24}$ film. The improvement in the soft magnetic properties is one of our future works.

## 4 Conclusion

The different atomic ratios of FeCo alloys were prepared with eco-friendly reducing agents arabinogalactan, starch, and sucrose. The thick films prepared with this simple and efficient method have a high magnetization close to the values in bulk Fe–Co alloys. The Fe–Co coatings are nanocrystalline bcc solid solution with carbon additive no more than 2 at% in alloys with Co content from 0 to 90 at%. It has been shown that the type of polysaccharide determines the deposition rate and grain size in the films. The smallest grain size (~ 12 nm) is observed for films produced with arabinogalactan. The highest deposition rate of the FeCo film was fixed for series C (50 nm/s). For $Fe_{70}Co_{30}$ films reduced with carbohydrates, the $M_s$ values are 205, 235, and 240 emu/g for arabinogalactan, starch, and sucrose, respectively. Surface relief, columnar microstructure, and hysteresis loops are controlled by varying reducing agents and Co contents. The positive linear correlation of the Co content in Fe–Co alloy and the local magnetic anisotropy field is observed.

**Acknowledgements** The authors thank the Krasnoyarsk Regional Center of Research Equipment of Federal Research Center "Krasnoyarsk Science Center SB RAS" for the provided equipment. We are grateful to Yu.L. Mikhlin for the X-ray photoelectron spectral analysis. The authors thank M. Volochaev for the transparent electron microscopy images. We are grateful to M. Rautsky for his contribution in obtaining ferromagnetic resonance experimental data. The authors are thankful to E.V. Grigoriev for performing of XRD measurements.

**Funding** This work was funded by the Russian Foundation for Basic Research, Krasnoyarsk Territory, and Krasnoyarsk Regional Fund of Science, project number 20–43-240003.

**Availability of Data and Materials** Data available on request from the authors.

## Declarations

**Conflict of Interest** The authors declare no competing interests.

## References

1. Osaka, T.: Electrodeposition of highly functional thin films for magnetic recording devices of the next century. Electrochim. Acta. **45**, 3311–3321 (2000). https://doi.org/10.1016/S0013-4686(00)00407-2
2. Alper, M., Kockar, H., Sahin, T., Karaagac, O.: Properties of Co–Fe films: dependence of cathode potentials. IEEE Trans. Magn. **46**, 390–392 (2010). https://doi.org/10.1109/TMAG.2009.2033711
3. Han, M., Lu, H., Deng, L.: Control of gigahertz permeability and permittivity dispersion by means of nanocrystallization in FeCo based nanocrystalline alloy. Appl. Phys. Lett. **97**, 192507 (2010). https://doi.org/10.1063/1.3514557
4. Cheng, Y., Ji, G., Li, Z., Lv, H., Liu, W., Zhao, Y., Cao, J., Du, Y.: Facile synthesis of FeCo alloys with excellent microwave absorption in the whole Ku-band: effect of Fe/Co atomic ratio. J. Alloys Compd. **704**, 289–295 (2017). https://doi.org/10.1016/j.jallcom.2017.02.024
5. Amsarajan, S., Jagirdar, B.R.: Air-stable magnetic cobalt-iron ($Co_7Fe_3$) bimetallic alloy nanostructures via co-digestive ripening of cobalt and iron colloids. J. Alloys Compd. **816**, 152632 (2020). https://doi.org/10.1016/j.jallcom.2019.152632
6. Yanai, T., Shiraishi, K., Watanabe, Y., Ohgai, T., Nakano, M., Suzuki, K., Fukunaga, H.: Magnetic Fe-Co films electroplated in a deep-eutectic-solvent-based plating bath. J. Appl. Phys. **117**, 17A925 (2015). https://doi.org/10.1063/1.4918782
7. Bautin, V.A., Kholodkov, N.S., Seferyan, A.G., Usov, N.A.: Chemically synthesized FeCo powder for advanced applications. J. Supercond. Nov. Magn. **31**, 3371 (2018)
8. Rizal, C., Kolthammer, J., Pokharel, R.K., Choi, B.C.: Magnetic properties of nanostructured Fe-Co alloys. J. Appl. Phys. **113**, 113905 (2013). https://doi.org/10.1063/1.4795267
9. Sun, K., Wang, K., Yu, T., Liu, X., Wang, G., Jiang, L., Bu, Y., Xie, G.: High-performance Fe Co P alloy catalysts by electroless deposition for overall water splitting. Int. J. Hydrog. Energy. **44**, 1328–1335 (2019). https://doi.org/10.1016/j.ijhydene.2018.11.182

10. Liu, X., Morisako, A.: Magnetic properties of FeCo films prepared by co-sputtering and hydrogenous gas reactive sputtering. IEEE Trans. Magn. **44**, 3910–3912 (2008). https://doi.org/10.1109/TMAG.2008.2001349
11. Reichel, L., Giannopoulos, G., Kauffmann-Weiss, S., Hoffmann, M., Pohl, D., Edström, A., Oswald, S., Niarchos, D., Rusz, J., Schultz, L., Fähler, S.: Increased magnetocrystalline anisotropy in epitaxial Fe-Co-C thin films with spontaneous strain. J. Appl. Phys. **116**, 213901 (2014). https://doi.org/10.1063/1.4901595
12. Maklakov, S.S., Maklakov, S.A., Ryzhikov, I.A., Amelichev, V.A., Pokholok, K.V., Lagarkov, A.N.: Mössbauer study of disordering in thin sputtered FeCo–$SiO_2$ and FeCo films. J. Alloys Compd. **536**, 33–37 (2012). https://doi.org/10.1016/j.jallcom.2012.05.022
13. Mehrizi, S., Heydarzadeh Sohi, M.: Electrical resistivity and magnetic properties of electrodeposited nanocrystalline CoFe thin films. J. Mater. Sci. Mater. Electron. **26**, 7381–7389 (2015). https://doi.org/10.1007/s10854-015-3368-6
14. Iskhakov, R.S., Chekanova, L.A., Denisova, E.A.: Magnitic properties of electroless fine Co-P particles. IEEE Trans. Magn. **33**, 3730–3732 (1997). https://doi.org/10.1109/20.619553
15. Vazenina, I.G., Iskhakov, R.S., Stolyar, S.V., Chekanova, L.A.: Spin-wave resonance in one-dimensional magnonic crystals by an example of multilayer Co–P films. Phys. Solid State. **62**, 1861–1867 (2020). https://doi.org/10.1134/S1063783420100121
16. Chang, P.R., Yu, J., Ma, X., Anderson, D.P.: Polysaccharides as stabilizers for the synthesis of magnetic nanoparticles. Carbohydr. Polym. **83**, 640–644 (2011). https://doi.org/10.1016/j.carbpol.2010.08.027
17. Machado, S., Pinto, S.L., Grosso, J.P., Nouws, H.P.A., Albergaria, J.T., Delerue-Matos, C.: Green production of zero-valent iron nanoparticles using tree leaf extracts. Sci. Total Environ. **445–446**, 1–8 (2013). https://doi.org/10.1016/j.scitotenv.2012.12.033
18. Sukhov, B.G., Aleksandrova, G.P., Grishchenko, L.A., Feoktistova, L.P., Sapozhnikov, O.A., Proidakova, N.A., T'kov, A.V., Medvedeva, S.A., Trofimov, B.A.: Nanobiocomposites of noble metals based on arabinogalactan: preparation and properties. J. Struct. Chem. **48**, 922–927 (2007). https://doi.org/10.1007/s10947-007-0136-3
19. Takata, F.M., Sumodjo, P.T.A.: Electrodeposition of magnetic CoPd thin films: influence of plating condition. Electrochim. Acta. **52**, 6089–6096 (2007). https://doi.org/10.1016/j.electacta.2007.03.048
20. Herzer, G.: Grain size dependence of coercivity and permeability in nanocrystalline ferromagnets. IEEE Trans. Magn. **26**, 1397–1402 (1990). https://doi.org/10.1109/20.104389
21. Denisova, E.A., Chekanova, L.A., Komogortsev, S.V., Nemtsev, I.V., Iskhakov, R.S.: Structure and magnetic properties of the FeCo-C films reduced by carbohydrates. Semiconductors **54**, 1840–1842 (2020). https://doi.org/10.1134/S1063782620140079
22. Lu, W., Huang, P., He, C., Yan, B.: Compositional and structural analysis of FeCo films electrodeposited at different temperatures. Int. J. Electrochem. Sci. **7**, 12262–12269 (2012)
23. Aleksandrova, G.P., Boymirzaev, A.S., Klimenkov, I.V., Sukhov, B.G., Trofimov, B.A.: Modification of the arabinogalactan matrix in the formation of metal-polymer nanobiocomposites. Nanotechnol. Russ. **14**, 41–47 (2019). https://doi.org/10.1134/S1995078019010026
24. Nik Rozlin, N.M., Alfantazi, A.M.: Nanocrystalline cobalt–iron alloy: synthesis and characterization. Mater. Sci. Eng. A. **550**, 388–394 (2012). https://doi.org/10.1016/j.msea.2012.04.092
25. Wijn, H.P.J.: Magnetic properties of metals d-elements. Alloys and Compounds (Data in Science and Technology). Springer (1991)
26. Bozorth, R.M.: Ferromagnetism. D. Van Nostrand, New York (1951)
27. Koza, J.A., Uhlemann, M., Gebert, A., Schultz, L.: The effect of magnetic fields on the electrodeposition of CoFe alloys. Electrochim. Acta. **53**, 5344–5353 (2008). https://doi.org/10.1016/j.electacta.2008.02.082
28. Denisova, E., Chekanova, L., Nemtsev, I., Komogortsev, S., Shepeta, N.: Soft magnetic FeCo films produced by green chemistry technique. J. Phys. Conf. Ser. **1582**, 012077 (2020). https://doi.org/10.1088/1742-6596/1582/1/012077
29. Parette, G., Mirebeau, I.: Magnetic moment distribution in iron-cobalt alloys. Phys. B Condens. Matter. **156–157**, 721–723 (1989). https://doi.org/10.1016/0921-4526(89)90773-4
30. Yanai, T., Mieda, K., Kaji, J., Tanaka, R., Yamashita, A., Morimura, T., Nakano, M., Fukunaga, H.: Electroplated Fe-Co films prepared in citric-acid-based plating baths with saccharin and sodium lauryl sulfate. AIP Adv. **10**, 5–5001 (2020). https://doi.org/10.1063/1.5130468
31. Kitamoto, Y., Tagami, H., Kiyota, G.: Microstructural and magnetic study of nanocrystalline soft magnetic thin films of Fe–C and Fe–Co–C deposited with sputtering. IEEE Trans. Magn. **41**, 3295–3297 (2005). https://doi.org/10.1109/TMAG.2005.854719
32. Cao, D., Cheng, X., Feng, H., Jin, C., Zhu, Z., Pan, L., Wang, Z., Wang, J., Liu, Q.: Investigation on the structure and dynamic magnetic properties of FeCo films with different thicknesses by vector network analyzer and electron spin resonance spectroscopy. J. Alloys Compd. **688**, 917–922 (2016). https://doi.org/10.1016/j.jallcom.2016.07.110
33. Kittel, C.: On the theory of ferromagnetic resonance absorption. Phys. Rev. **73**, 155–161 (1948). https://doi.org/10.1103/PhysRev.73.155
34. Iskhakov, R.S., Komogortsev, S.V.: Magnetic microstructure of nanostructured ferromagnets. Bull. Russ. Acad. Sci. Phys. **71**, 1620–1622 (2007). https://doi.org/10.3103/S1062873807110470
35. Zhang, Y., Ivey, D.G.: Characterization of Co–Fe and Co–Fe–Ni soft magnetic films electrodeposited from citrate-stabilized sulfate baths. Mater. Sci. Eng. B. **140**, 15–22 (2007). https://doi.org/10.1016/j.mseb.2007.03.004